CARBON ENERGY WILEY

Graphene-based catalysts for electrochemical carbon dioxide reduction

Amirhossein Hasani[1] | **Mahider Asmare Teklagne[1]** | **Ha Huu Do[1,2,3]** | **Sung Hyun Hong[2]** | **Quyet Van Le[3]** | **Sang Hyun Ahn[1]** | **Soo Young Kim[2]** 🔵

[1]School of Chemical Engineering and Materials Science, Integrative Research Center for Two-Dimensional Functional Materials, Institute of Interdisciplinary Convergence Research, Chung-Ang University, Seoul, Republic of Korea

[2]Department of Materials Science and Engineering, Korea University, Seoul, Republic of Korea

[3]Institute of Research and Development, Duy Tan University, Da Nang, Vietnam

Correspondence
Soo Young Kim, Department of Materials Science and Engineering, Korea University, 145 Anam-ro, Seongbuk-gu, Seoul 02841, Republic of Korea.
Email: sooyoungkim@korea.ac.kr

Abstract

Electrochemical carbon dioxide (CO_2) reduction is considered to be an efficient strategy to produce usable fuels and overcome the concerns regarding global warming. For this purpose, an efficient, earth abundant, and a low cost catalyst has to be designed. It has been found that graphene-based materials could be promising candidates for CO_2 conversion because of their unique physical, mechanical, and electronic properties. In addition, the surface of graphene-based materials can be modified by using different strategies, including doping, defect engineering, producing composite structures, and wrapping shapes. In this review, the fundamentals of electrochemical CO_2 reduction and recent progress of graphene-based catalysts are investigated. Furthermore, recent studies on graphene-based materials for CO_2 reduction are summarized.

KEYWORDS
catalyst, CO_2 reduction, electrochemical, graphene

1 | INTRODUCTION

The development of industrialization in the world leads to an increase in temperature owing to the emission of redundant gases such as carbon dioxide (CO_2) to the atmosphere.[1] In addition, the energy consumption is expected to reach approximately two times the current energy consumption by 2050.[2] To avoid these consequences and decrease the atmospheric CO_2 concentration, the direct electroreduction of CO_2 can be employed to reduce the CO_2 emission, and the accumulation from various sources into materials that can be used as a fuel source should be decreased.[3-6] Electroreduction is advantageous because (a) it is environmentally compatible with the carbon-free renewable energy resources (solar and wind), (b) it operates under ambient temperature and pressure, (c) reactions can be controlled by adjusting the external conditions such as electrolytes and applied voltages, and (d) it is feasible in terms of engineering and economics. However, this process has been extremely challenging for a long time, and continues to be because of the large overpotential required for dissociation of C=O

bond, slow electron transfer kinetics, low selectivity, and low stability.

For this process to become economically viable, different technological advances have to be made. Much of the early work focused on exploring different catalysts and products that can be produced. Different types of catalysts that can catalyze the CO_2 reduction reaction have been synthesized and studied. Transition metals such as Pt, Rh, Ag, Au, and Ni, which have vacant orbits and active d electrons,[7,8] oxides (RuO_2[9] and IrO_2[10]), chalcogenides,[11] carbides,[12] and metal organic frameworks[13] have shown potential as catalysts for CO_2 reduction.

Recently, graphene, two-dimensional layers of sp^2-bonded carbon arranged in a honeycomb lattice, has received extensive attention as an electrode in different applications such as electrochemical devices, lithium-ion batteries, and fuel cells.[14,15] It has a large surface area, high carrier mobility, high thermal conductivity, and high current and heat conduction.[16,17] Many methods have been reported for the synthesis of graphene and graphene-based materials, such as the mechanical cleavage of graphite,[18] chemical exfoliation of graphite,[19] solvothermal synthesis,[20] and chemical vapor deposition.[21] Studies have shown that pristine graphene has a low performance toward CO_2 reduction because of the neutral carbon atom. Theoretical and experimental studies have revealed that doping graphene with heteroatoms such as boron, nitrogen, and phosphorous can alter its electronic property and chemical reactivity, as well as give rise to new functions that can enhance the catalytic performance toward CO_2 reduction.[22-24] It should be noted that the rational design of these graphene-based nanomaterials with well-defined morphology also plays an important role in their performance toward CO_2 reduction. Furthermore, the unique properties of graphene and its hybrid materials and the ease of processibility make them ideal candidates for a variety of energy applications. The properties of graphene in composite materials are different from that of bare graphene owing to the defective, oxygenated functional groups and aggregation of the graphene sheets.[25,26]

Graphene has a lot of advantages compared with other relative materials such as CNT and g-C_3N_4, including high electron mobility at room temperature, excellent thermal conductivity, and superior mechanical properties with a high Young modulus.[1] Besides, band gap of graphene can be tuned to produce semiconductive graphene which can used in transistors and as a catalyst. In addition, graphene can be modified further by engineering its shape, size, and chemical structure to expand its application. The different synthesis methods of graphene such as solution processing also allow graphene not only for using in an electronic device but also a new

area in optoelectronic such as solar cells and photoelectrochemical water splitting.[22-24]

This mini-review will attempt to elucidate the use of graphene-based electrocatalyst and photocatalyst in the reduction of CO_2 to usable fuels. First, we will briefly discuss the fundamental mechanism of CO_2 reduction followed by the methods used to modify the structure and properties of graphene, and the role of graphene in each composite structure with selected examples.

2 | CO_2 REDUCTION

2.1 | Fundamentals of CO_2 electrolysis

The process of electrochemical CO_2 reduction occurs at the interface of electrolyte and electrodes, and it can mainly be expressed by the following steps[27]:

(1) Absorption of CO_2 on the catalyst surface.
(2) Formation of C–H bonds and breaking of C–O bonds via proton and electron transfer.
(3) Desorption and formation of new products at the electrode, and diffusion of these products into the electrolyte from the surface.

The proton reduction can be an obstacle in transferring electrons; this limits the selectivity for organic products, and could be a hindrance for CO_2 reduction. In addition, the diffusion reactions can be affected by the low solubility of CO_2 in electrolytes. However, we can overcome these challenges by different ways, including operating at low temperature, using nonaqueous electrolyte, and increasing CO_2 concentration. Thermodynamically, some metal catalysts cannot enhance the reaction in ambient pressure. Therefore, the CO_2 reduction and formation of organic compounds have to be achieved in as-increased partial pressure. Moreover, the selectivity and rate of reactions can be enhanced by increasing CO_2 flow rate.[28]

Furthermore, certain parameters can be used to evaluate the catalytic performance: current density, overpotential, onset potential, Tafel slope, faradaic efficiency (FE), and turnover frequency (TOF).[27]

2.1.1 | Current density

The basic principle of the electrochemical process is the electron transfer between the electrodes and electrolyte, and this transfer is considered to be dimensionally homogeneous. Therefore, the amount of current per unit area should be considered as a parameter for figure of merit.[29]

2.1.2 | Overpotential

The overpotential is the voltage difference between the actual reaction potential and thermodynamic potential. In fact, a constant potential is required by a specific ion in the redox reaction. To react, the ions need to move from the bulk of the electrolyte to the electrode interface. However, ions have to overcome a resistance due to collisions with each other. Therefore, an extra voltage, which is the overpotential, needs to be applied.[30]

2.1.3 | Onset potential

The onset potential is the voltage required to increase the current and start the reaction. An efficient catalyst decreases the amount of onset potential, thereby decreasing the power consumption.

2.1.4 | Tafel slope

The relationship between the rate of electrochemical reaction and overpotential can be expressed by using the Tafel equation in an electrochemical process. In addition, studies on the corrosion and open circuit voltage can be carried out by using the Tafel curve.[30]

2.1.5 | Faradaic efficiency

FE is utilized to evaluate the efficiency and selectivity of an electrochemical reaction, and can be expressed by the following equation:
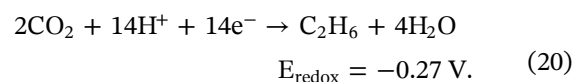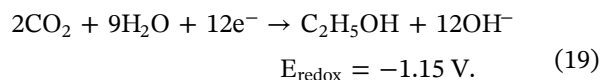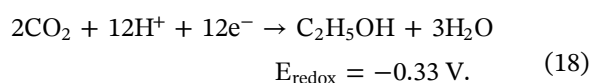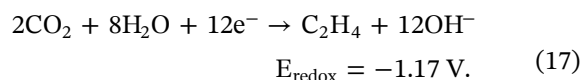
$$FE = \frac{z \times n \times F}{I \times t} \times 100, \tag{1}$$

where z is the number of electrons, n is the molar ratio of product, I is the applied current, t is the duration of the reaction, and F is the Faraday constant.

2.2 | Thermodynamics of CO_2 reduction

The formation of CO_2 anion radical is related to the electron transfer process. Because of a high negative redox potential, the electron transfer is quite impossible. For this reason, catalysts are introduced to reduce the number of CO_2 anion radicals via electron and proton transfer at an extremely low potential in an efficient way.

In fact, the number of transferred protons and electrons determine the products of CO_2 reduction.[27,31] The possible reactions are shown in the following:

$$CO_2 + 2H^+ + 2e^- \rightarrow HCOOH \quad E_{redox} = 0.61 \text{ V.} \tag{2}$$

$$CO_2 + 2H_2O + 2e^- \rightarrow HCOOH^- + 2OH^-$$
$$E_{redox} = -1.5 \text{ V.} \tag{3}$$

$$CO_2 + 2H^+ + 2e^- \rightarrow CO + H_2O \quad E_{redox} = -0.53 \text{ V.} \tag{4}$$

$$2CO_2 + 2H_2O + 2e^- \rightarrow 2CO + 4OH^-$$
$$E_{redox} = -1.34 \text{ V.} \tag{5}$$

$$2CO_2 + 2H^+ + 2e^- \rightarrow H_2C_2O_4 \quad E_{redox} = -0.91 \text{ V.} \tag{6}$$

$$2CO_2 + 2e^- \rightarrow C_2O_4^{2-} \quad E_{redox} = -1 \text{ V.} \tag{7}$$

$$CO_2 + 4H^+ + 4e^- \rightarrow HCHO + H_2O \quad E_{redox} = -0.5 \text{ V.} \tag{8}$$

$$CO_2 + 3H_2O + 4e^- \rightarrow HCHO + 4OH^-$$
$$E_{redox} = -1.31 \text{ V.} \tag{9}$$

$$CO_2 + 4H^+ + 4e^- \rightarrow C + 2H_2O \quad E_{redox} = -0.2 \text{ V.} \tag{10}$$

$$CO_2 + 2H_2O + 4e^- \rightarrow C + 4OH^- \quad E_{redox} = -1.04 \text{ V.} \tag{11}$$

$$CO_2 + 6H^+ + 6e^- \rightarrow CH_3OH + H_2O$$
$$E_{redox} = -0.3 \text{ V.} \tag{12}$$

$$CO_2 + 5H_2O + 6e^- \rightarrow CH_3OH + 6OH^-$$
$$E_{redox} = -1.22 \text{ V.} \tag{13}$$

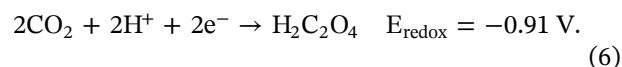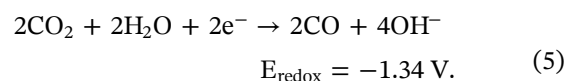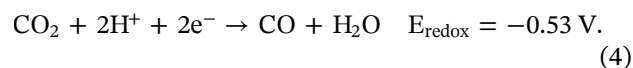$$CO_2 + 8H^+ + 8e^- \rightarrow CH_4 + 2H_2O \quad E_{redox} = -0.24 \text{ V.} \tag{14}$$

$$CO_2 + 6H_2O + 8e^- \rightarrow CH_4 + 8OH^-$$
$$E_{redox} = -1.22 \text{ V.} \tag{15}$$

$$2CO_2 + 12H^+ + 12e^- \rightarrow C_2H_4 + 4H_2O$$
$$E_{redox} = -0.35 \text{ V.} \tag{16}$$

$$2CO_2 + 8H_2O + 12e^- \rightarrow C_2H_4 + 12OH^-$$
$$E_{redox} = -1.17 \text{ V.} \tag{17}$$

$$2CO_2 + 12H^+ + 12e^- \rightarrow C_2H_5OH + 3H_2O$$
$$E_{redox} = -0.33 \text{ V.} \tag{18}$$

$$2CO_2 + 9H_2O + 12e^- \rightarrow C_2H_5OH + 12OH^-$$
$$E_{redox} = -1.15 \text{ V.} \tag{19}$$

$$2CO_2 + 14H^+ + 14e^- \rightarrow C_2H_6 + 4H_2O$$
$$E_{redox} = -0.27 \text{ V.} \tag{20}$$

$$2CO_2 + 9H_2O + 12e^- \rightarrow C_2H_5OH + 12OH^-$$
$$E_{redox} = -1.15 \text{ V.} \qquad (21)$$

$$3CO_2 + 18H^+ + 18e^- \rightarrow C_3H_7OH + 5H_2O$$
$$E_{redox} = -0.31 \text{ V.} \qquad (22)$$

$$2H^+ + 2e^- \rightarrow H_2 \quad E_{redox} = -0.42 \text{ V.} \qquad (23)$$

The aforementioned reactions depend on different factors, including the temperature, type of electrolyte, properties of catalyst (eg, crystal structure, electronic properties, size, elemental composition, etc), electrolyte pH, and applied voltage. According to the Gibbs free energy relation ($\Delta G = -nFE^0$), a reduction reaction occurs when E^0 is positive. Here, n is the number of transferred electrons during the oxidation and reduction, and F is the FE. In addition, the CO_2 reduction depends thermodynamically on the concentrations of the electron and proton in the electrolyte. The selectivity of C_2 and other hydrocarbon products can be limited by the fact that the hydrogenation of attached C_1 is more facile than the C–C bond formation. Moreover, the catalytic efficiency may be restricted by the energy of adsorption in a CO_2 reduction reaction. However, to enhance the catalytic performance, a study on decreasing coordination number, doping, and deposition of the catalyst surface with the ligands has to be conducted.[32]

2.3 | Electrolytes

In an electrochemical CO_2 reduction, an electrolyte provides a platform for transferring the electrons and protons, and the catalytic activity is related to the concentration and type of electrolyte. In addition, some factors such as the catalyst active sites and impurities can affect the catalytic performance. The electrolytes can be categorized into four types: (a) aqueous, (b) ionic, (c) organic, and (d) solid.[27]

2.3.1 | Aqueous electrolytes

Studies on electrochemical CO_2 reduction have been extensively carried out with aqueous electrolytes. Aqueous electrolytes include an alkali or poorly acidic CO_2-saturated solution, and contain metal cations and inorganic salt anions such as Cl^-, SO_4^{2-}, HCO_3, Na^+, and K^+.[33] The cations can affect the current density and selectivity as they influence the concentration of charged anions near the electrodes. In addition, the size of cations has an impact on the products generated by electrochemical CO_2 reduction. In contrast, the anionic species can alter the pH of electrolyte and enhance the selectivity and catalytic activity. Hydrogen evolution can be restricted by the low concentration of protons caused by increasing pH. Volatile organic compounds and ethylene are preferably generated by using $KHCO_3$, KCl, and $KClO_4$ in an electrolyte with high pH. In contrast, methane (CH_4) is favored to be produced by using the saturated $KHCO_3$ electrolytes. For example, Ogura et al[34] investigated the electrochemical CO_2 reduction on a copper (Cu) mesh in an aqueous electrolyte including 3M of KCl, KI, and KBr. Cu can facilitate the electron transfer from the electrode to the electrolyte; this process likely occurs through the Cl^-–C bond, and results in the transfer of electron from the absorbed anion to the vacant CO_2 orbitals. Thus, the rate of halide anion absorption is much higher than that of proton adsorption, suggesting an increase in overpotential for H_2 evolution. Therefore, the addition of halide anions like Br^- and Cl^- can improve the selectivity of the CO product. In contrast, the presence of Cl^- reduces the CO selectivity as the CH_4 composition formed is higher than the electrolyte that does not contain halides.[35]

2.3.2 | Ionic electrolytes

Ionic solutions containing imidazolium cations can provide some advantages: the decrease in electrochemical CO_2 reduction overvoltage by decreasing the energy of CO_2^- intermediates, prevention of hydrogen production, and enhancement of the selectivity of products. For example, Sun et al[36] fabricated a catalyst based on an N-doped graphene/carbon paper electrode in an ionic electrolyte for electrochemical CO_2 reduction. As a result, they achieved a very high FE of 93.5% toward CH_4. In addition, the effect of H_2O on electrolysis was investigated as shown in Figure 1A. The ionic electrolyte increased the current density and stability (see Figure 1B). In addition, Figure 1C,D indicate the dependencies of FE and partial current density on the applied voltage, respectively for different water contents in ionic electrolyte. The mechanism of electrochemical reduction of CO_2 to CH_4 is shown schematically in Figure 1E. First, the CO_2 is adsorbed onto the N binding sites, where CO_2 is reduced ($CO_2^{\cdot-}$). Here, the [Bmim]BF_4 aids the formation of CO_2^-. Subsequently, the CO_2^- is conjugated, and the acidic CO_2 molecules decompose to CO_2–CO_2^- (Step 3). In Step 4, energy is applied thermodynamically to transfer the electrons and form CO_{ads}. In Step 5, the as-adsorbed CO can be detached and transformed to CHO by accepting a proton and an electron. Finally, CH_4 is formed by the addition of more electrons and protons.[36]
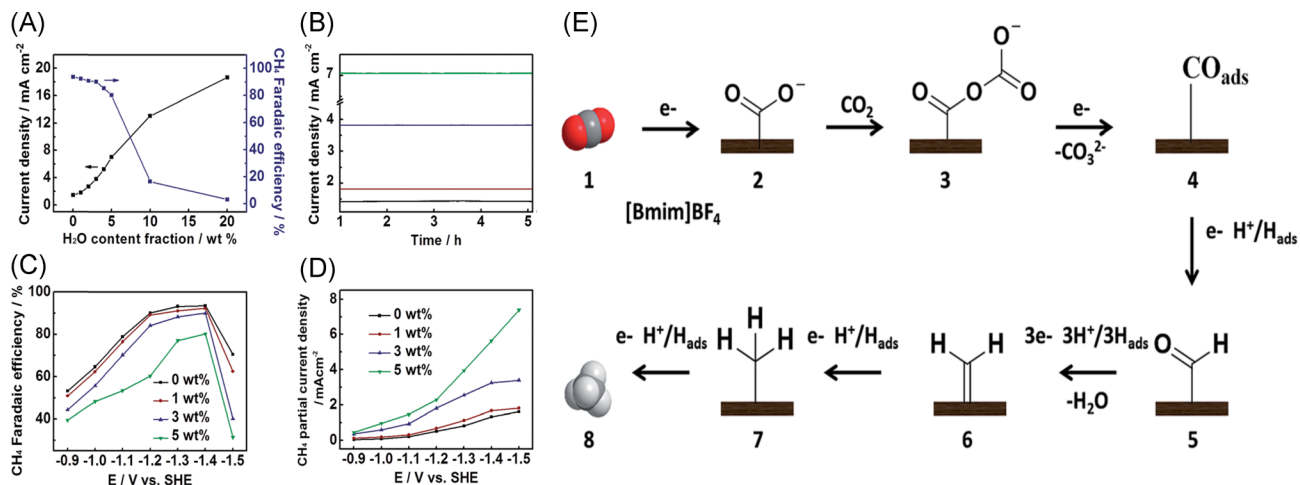
FIGURE 1 The catalytic performance of the NGM-1/CP electrode in CO_2 electrochemical reduction using [Bmim]BF$_4$–H$_2$O binary electrolytes. A, The effect of water content on the current density at an applied potential of −1.400 V. B, Time curves of the electrolysis processes at water contents of 0, 1, 3, and 5 wt% (from bottom to top) at −1.400 V. C, Dependence of the FEs of CH_4 on the applied potential at different water contents. D, Dependence of the partial current densities of CH_4 on the applied potential at different water contents. FEs, Faradaic efficiencies. Reproduced with permission: Copyright 2016, Wiley.[36]

2.3.3 | Organic electrolytes

To enhance the FE and solubility of CO_2, a nonaqueous solution can be utilized as the electrolyte. For example, CO_2 can be dissolved easily in DMF and propylene carbonate, which are drastically better than an aqueous electrolyte. In addition, Vassiliev et al[35] showed that the dimerization of CO_2^- was facilitated by nonaqueous solvents via adsorption of CO_2 on Hg, Sn, and In

electrodes. Moreover, the CO_2 reduction performance can be tuned by adding water in organic solutions.

2.4 | Experimental electrochemical cell for CO_2 reduction

As there is neither a specific experimental setup nor a standard method for electrochemical CO_2 reduction,
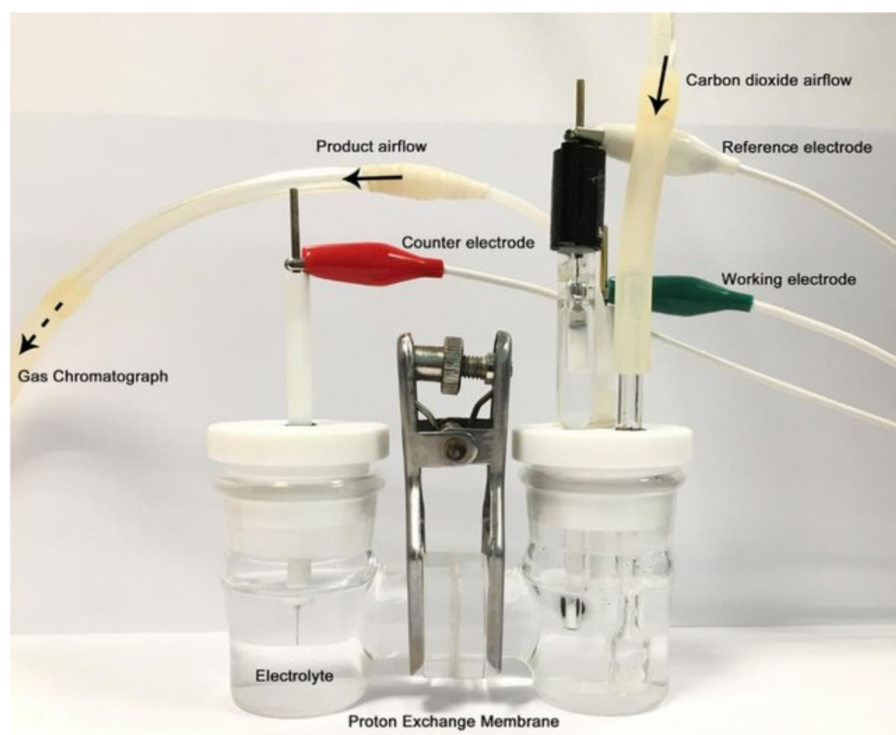

FIGURE 2 H-type electrolytic cell used for electrochemical tests. Reproduced with permission: Copyright 2018, American Chemical Society.[38]
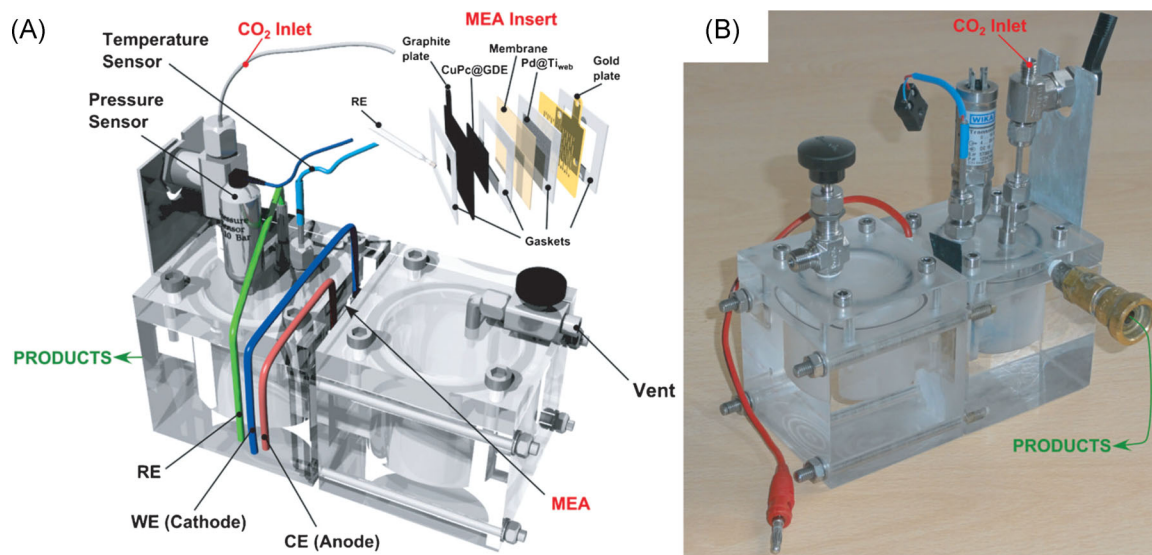
FIGURE 3 A, Schematic of the depolarized anode alkaline membrane CO_2 electrolyzer and (B) a photograph of its practical realization. Reproduced with permission: Copyright 2014, Wiley.[41]

various experimental setups have been proposed for CO_2 reduction. However, two main electrochemical experimental setups, namely the H-shaped cell and continuous cell have been used frequently.[27,37] The most common lab-made electrochemical cell is the H-type cell, including three components: working, counter, and reference electrodes. Figure 2 shows a practical H-type electrochemical cell.[38] From Figure 2, it is evident that the anodic and cathodic parts of the cell are separated by a membrane (eg, Nafion or a polymer), which aids the proton-transfer. Although the anodic and cathodic parts are placed close to each other in the H-type electrochemical setup, the transfer of generated products from the cathode is prevented; in addition, the ions can move

easily through the electrolyte. Further, the cathodic part is connected to the analyses equipment (eg, gas chromatography) to detect the as-generated products. Recently, the continuous-flow electrochemical cell has also been applied for the analysis of electrochemical CO_2 reduction.[39,40] For example, Bevilacqua et al[41] fabricated an electrolyzer device based on microfluidic flow cell for CO_2 reduction, and produced some useful hydrocarbons such as CH_4 and C_2H_4. Figure 3 illustrates the structure of a typical continuous cell. This setup consists of conductive gold and graphite parts, which represent the cathode and anode, respectively. Similar to the H-type cell, the cathodic part is directly connected to a gas chromatographer to analyze the generated products.
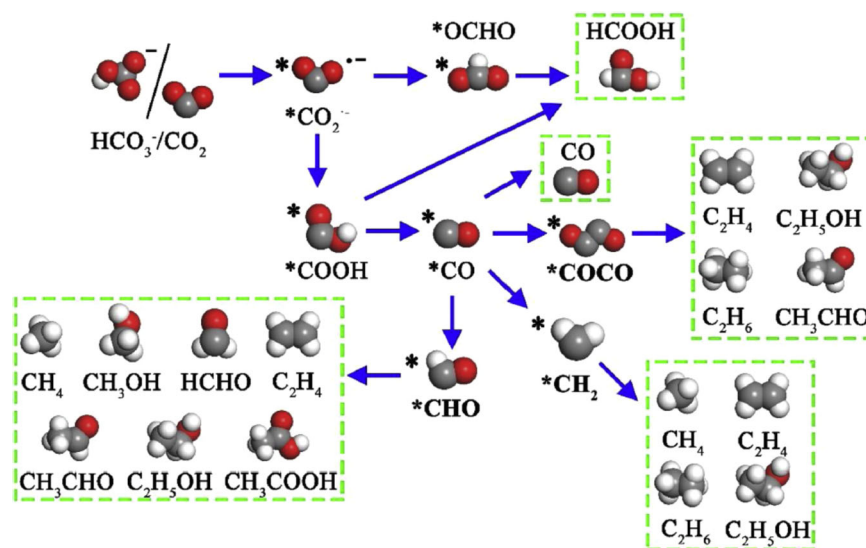

FIGURE 4 Proposed reaction pathways with key intermediates for different CO_2 electroreduction products. Reproduced with permission: Copyright 2019, Elsevier.[37]
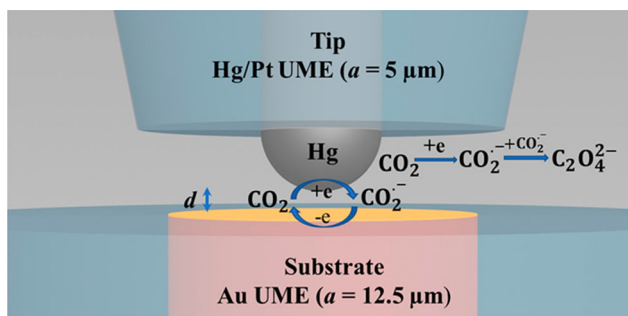
FIGURE 5 Schematic of the collection of the $CO_2{}^{\cdot-}$ radical in TG/SC mode of SECM. SECM, scanning electrochemical microscope. Reproduced with permission: Copyright 2017, American Chemical Society.[44]

In addition, an exhaust is provided in the cathodic part for the as-generated products to exit. Moreover, a depolarized alkali was used as the membrane. The maximum FE achieved for CH_4 by using this cell has been reported to be in between 80% and 90%.[40,41]

2.5 | Possible reactions and products

Researchers have been trying to understand the mechanism of CO_2 reduction. In fact, theoretical and experimental approaches have been combined to elucidate the reaction pathways of CO_2 reduction. However, most of the hypotheses are based on the experimental results (electrochemical results such as overpotential, Tafel slope, FE, and TOF) and computational methods (eg, density functional theory [DFT]). Therefore, to carry out an appropriate study to understand the CO_2

reduction mechanism, both experimental and theoretical results are required. Figure 4 shows all possible reaction pathways for different products, schematically.[37] The possible reactions that occur via intermediates are explained in the following.

2.5.1 | Formation of CO_2 radical anion ($CO_2{}^{\cdot-}$)

The initial step in electrochemical CO_2 reduction is to transfer the electrons to produce $CO_2{}^{\cdot-}$ anion radicals, and use a massive amount of energy to rearrange the CO_2 to $CO_2{}^{\cdot-}$ anion radicals, whose mechanism has been elaborated previously.[42] Several spectroscopic approaches such as Raman spectroscopy, scanning electrochemical microscopy, and Fourier-transform infrared spectroscopy have been used to explore the intermediates on the metal electrode interface.[43-45] For example, Kai et al[44] determined the CO_2 radicals ($CO_2{}^{\cdot-}$) quantitatively in DMF-based electrolyte by using a scanning electrochemical microscope (SECM) on a Hg/Au electrode and hemisphere-shaped Hg/Pt. The as-generated $CO_2{}^{\cdot-}$ anion radicals form oxalate and can be observed between the substrate and SECM tip nano gap (see Figure 5).

2.5.2 | Formation of formyloxyl (*OCHO)

Formic acid (HCOOH), CO, and CH_4 can be generated via *OCHO intermediates during CO_2 reduction. Yoo et al[46] suggested that there are two reaction pathways for the formation of *OCHO as shown in Figure 6.
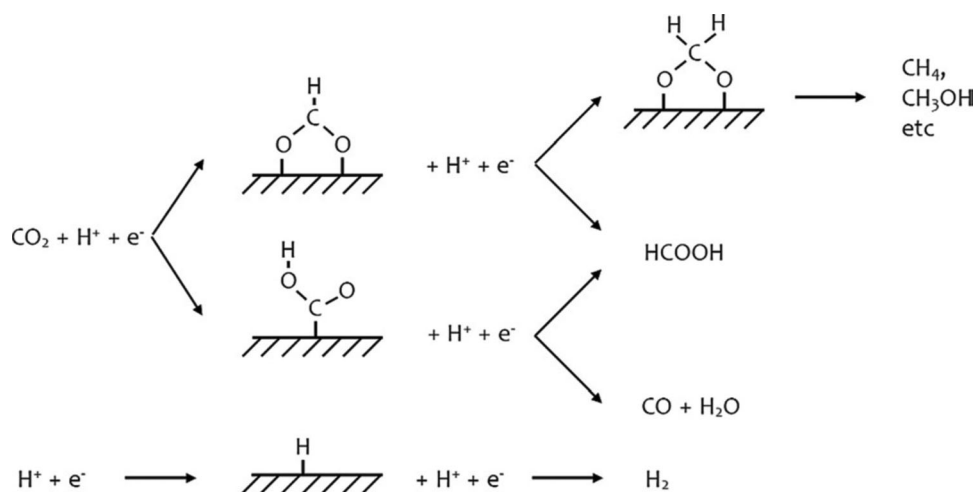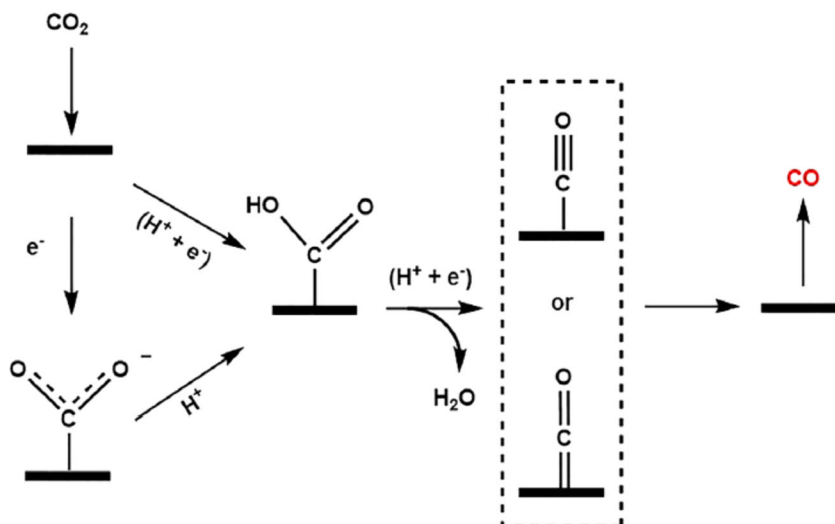

FIGURE 6 Reaction pathways for the electroreduction of CO_2 to different products (top), and the competing hydrogen evolution reaction (bottom). Reproduced with permission: Copyright 2016, Wiley.[46]

FIGURE 7 Possible reaction pathways for the electro-catalytic reduction of CO_2 to CO. Reproduced with permission: Copyright 2017, Elsevier.[27]

2.5.3 | Formation of carboxyl (*COOH)

CO can be generated via *COOH carboxyl intermediates, and the electron-proton transfer occurs based on the following reaction:

$$\text{*COOH} + \text{H}^+ + \text{e}^- \rightarrow \text{CO} + \text{H}_2\text{O}.$$
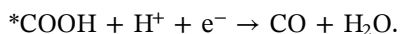
Chai et al[47] demonstrated that the formation of *COOH on N-doped graphene is more preferable than *OCHO based on DFT results.

2.5.4 | Formation of carbon monoxide

The electrochemical conversion of CO_2 to CO can be basically attributed to a paired electron transfer process as shown in Figure 7.[48] During the CO_2 reduction, a carboxyl intermediate (*COOH) is formed by the electron and proton transfer between the electrolyte and attached species. Then, H_2O and CO are formed via the OH group in *COOH by the absorption of H^+/e^- on the working electrode. *COOH can be converted to *CO easily. However, an extremely strong COOH bond can be an obstacle during the conversion of CO_2 to *COOH in the first step. This phenomenon is defined as the limiting rate of CO_2 reduction.[49] In addition, there is another way to produce *COOH; this can be done via the transfer of the separated proton and electron, followed by the formation of $CO_2^{\cdot 2-}$ radicals, which are adsorbed on the catalyst surface. Furthermore, pH plays a vital role in enhancing the generation of *COOH. In fact, the yield of *COOH increases as the pH increases.[24] The noble metals such as Pd, Ag, Au, and Zn can easily produce *CO intermediates. Moreover, *CO intermediates can form a weak bond with the working electrode surface; thus, CO can be detached easily from the electrode.[24,50,51]

2.5.5 | Formation of methane, methanol, and formaldehyde

It has been reported that *CO is a general intermediate for the generation of CH_4, HCHO, and CH_3OH. DFT calculations suggested that the Cu surface aids the formation of initial *CO intermediates thermodynamically, resulting in the hydrogenation of *HCO, *H$_3$CO, and *H$_2$CO. *O and CH_4 are the two productions of methoxy intermediate reduction. Finally, CH_4 and *O are converted to H_2O. The barriers for C–H formation and CH_3OH production are found to be 1.2 and 0.15 eV, respectively. In addition, *CHO intermediates can be reduced to C. This phenomenon was observed by using X-ray photoelectron spectroscopy and Auger electron spectroscopy during electrochemical measurement of working electrodes. Moreover, CH_4 can be produced via CH_3, CH_2, and CH_1 intermediates.

3 | GRAPHENE-BASED MATERIALS FOR CO_2 REDUCTION

In the last decades, carbon-based materials such as carbon nanotubes, graphene, and graphene oxide have been the focus of research because of their tunable, large surface area, and unique properties.[52-55] Specifically, graphene has been extensively studied, and its application in both electro- and photocatalytic CO_2 reduction has been investigated.

Many studies have attempted to design graphene-based catalysts for both electro- and photocatalytic CO_2 reduction. Because of the high electrical conductivity, graphene can facilitate the separation of charge carriers in photocatalytic CO_2 reduction. It is believed that the large contact area and strong interaction between
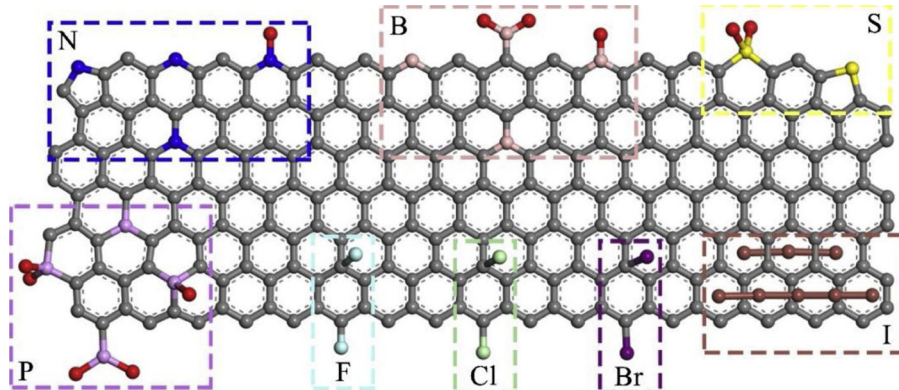
FIGURE 8 Illustration of doped graphene with different heteroatoms (B, N, S, P, F, Cl, Br, and I). Reproduced with permission: Copyright 2019, Elsevier.[37]

graphene and other catalysts promote photocatalytic reaction and improve CO_2 reduction performance.[56-58] For the electrocatalytic CO_2 reduction, pristine graphene and graphene oxide cannot be used in their natural form as they are inactive because of the presence of neutral carbon atom. Thus, graphene needs to be modified either by using heteroatom dopants such as boron, nitrogen, and phosphorus or by constructing graphene-based heterostructures to enhance its performance.

Studies have shown that graphene demonstrates better performance when it is hybridized with other materials and acted as support. In this case, the graphene should have the ability to provide a high surface for the materials or dopants to be dispersed and stabilized; completely.[1] To overcome this challenge, it requires to implement a method so-called defect-assisted doping, in which firstly a vacancy on the graphene surface should be created and subsequently the vacancies are filled with desired dopants. This process allows graphene to bind the atoms strongly, suggesting enhanced chemical reactivity as graphene acts as a support material. In addition, its large surface area and high conductivity can enable graphene to be used as a support for active surfaces such as nanosheets and nanoparticles (NPs) by accelerating charge transport and structural coupling effects.[52-55]

Surface modification is a key method used to enhance the performance of a material. Therefore, immense investigations have been carried out by modifying and tuning the surface of graphene to improve its performance. To modify the surface of graphene, methods such as doping, surface tuning, and composite structure have been introduced. Graphene modification can be achieved in two ways: covalent bonding and noncovalent interactions. The noncovalent modification processes include electrostatic interaction,[59] π–π stacking interactions,[60,61] the Van der waals force,[62] and hydrogen bonding.[63]
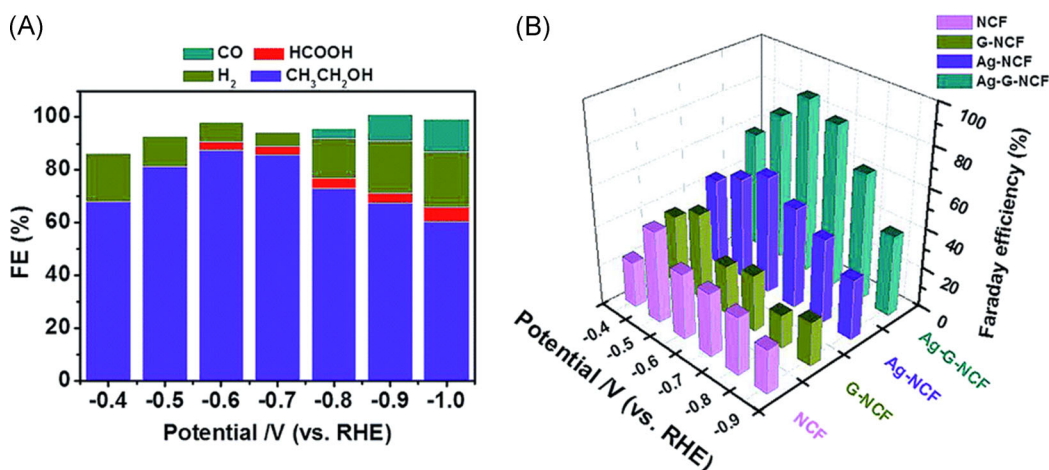
FIGURE 9 A, The FEs for acetate, ethanol, carbon monoxide, and hydrogen production obtained from the electrochemical reduction of CO_2 for 2 hours on an Ag-G-NCF electrode at −0.4 to −1.0 V vs RHE (0.1 M CO_2-saturated $KHCO_3$ aqueous solution). B, The FEs for ethanol on NCF, G-NCF, Ag-NCF, and Ag-G-NCF electrodes obtained from the electrochemical reduction of CO_2 for 2 hours at −0.4 to −0.9 V vs RHE (0.1 M CO_2-saturated $KHCO_3$ aqueous solution). FEs, FEs, Faradaic efficiencies; RHE, reversible hydrogen electrode. Reproduced with permission: Copyright 2018, The Royal Society of Chemistry.[73]
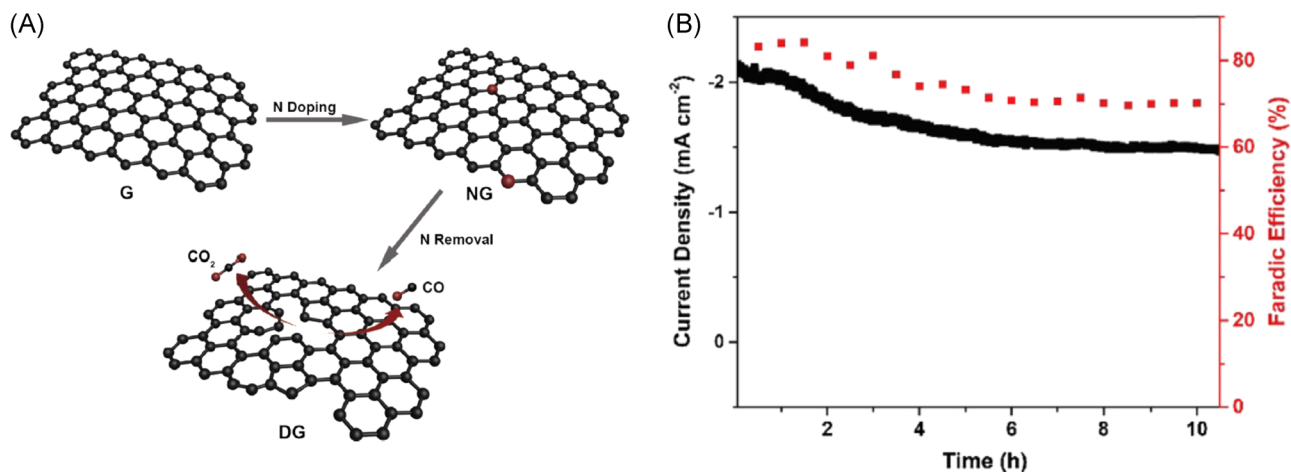
FIGURE 10 A, Schematic of the synthesis of defective graphene (DG), and the electrocatalytic reduction of CO_2 with DG. B, Time-dependent total current density curve (left y-axis) and FE (right y-axis) for the reduction of CO_2 to CO with DG in CO_2-saturated 0.1 M $KHCO_3$ solution at an applied potential of −0.6 V vs RHE for more than 10 hours. FE, Faradaic efficiency; RHE, reversible hydrogen electrode. Reproduced with permission: Copyright 2019, Elsevier.[74]

These modification processes are extremely easy, simple, and retains the natural graphene structure. The π–π stacking interactions are highly efficient among all the noncovalent modification methods. This method is highly advantageous in producing large surface area graphene.[64] Further, the covalent modification process involves the introduction of active double bonds and oxygen containing groups.[65] Stankovich et al[66] were the first to modify graphite oxide (GO) by using the covalent method. Isocyanate-treated GOs were synthesized by reacting the hydroxyl and carboxyl parts of GO with isocyanates. The generated product was extremely stable in different types of polar solvents. Amidation is another efficient method in covalent modification processes. Polymers such as polyethylenimine,[67] polyethylene glycol,[68] and poly(vinyl alcohol)[69] were used to modify the stability and hydrophilicity of graphene and GO.
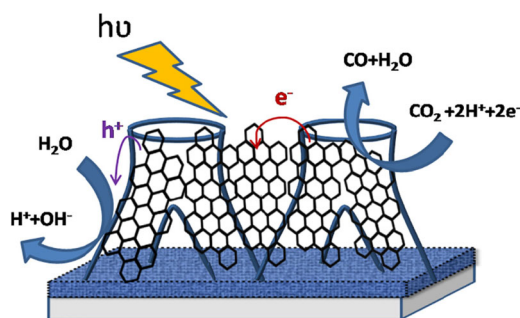

FIGURE 11 Schematic of the photocatalytic CO_2 reduction process involved in GO/rGO wrapped TiO_2 multileg nanotubes. GO, graphite oxide. Reproduced with permission: Copyright 2019, Elsevier.[75]

Furthermore, graphene can be modified using metallic and nonmetallic doping, surface tuning, and by making composite structures. Because of the large surface area of graphene, coupling graphene with other materials increases the active surface area; this is advantageous for CO_2 reduction.

Graphene-based materials could be easily modified with metallic and nonmetallic atoms as they have a long level of coordination atoms.[27] The binding energy of absorbed intermediates and breaking them could be obtained via alloying and combination of the different metal and nonmetal species, resulting in a decrease in over potential. In fact, some intermediates such as *CO prefer to bind to nonmetallic species via carbon atoms. In addition, doping is an efficient strategy to change the mechanical and electronic structure of graphene-based materials, suggesting in an enhancement in the selectivity of CO_2 reduction. Furthermore, functionalization of the graphene-based materials is an appropriate approach to enhance the catalytic activity and stability via H-bond and $CO_2^{.-}$ interaction.

3.1 | Doping

The reduction process cannot be efficiently performed with bare graphene because of the high absorption of CO_2 on the surface and the hindrance in forming carboxyl group in the initial step. Therefore, the catalytic properties should be tuned via metallic or nonmetallic doping; this can efficiently modify the graphene surface and catalytic properties that aid CO_2 reduction (see Figure 8). The doping can enhance the electrical and
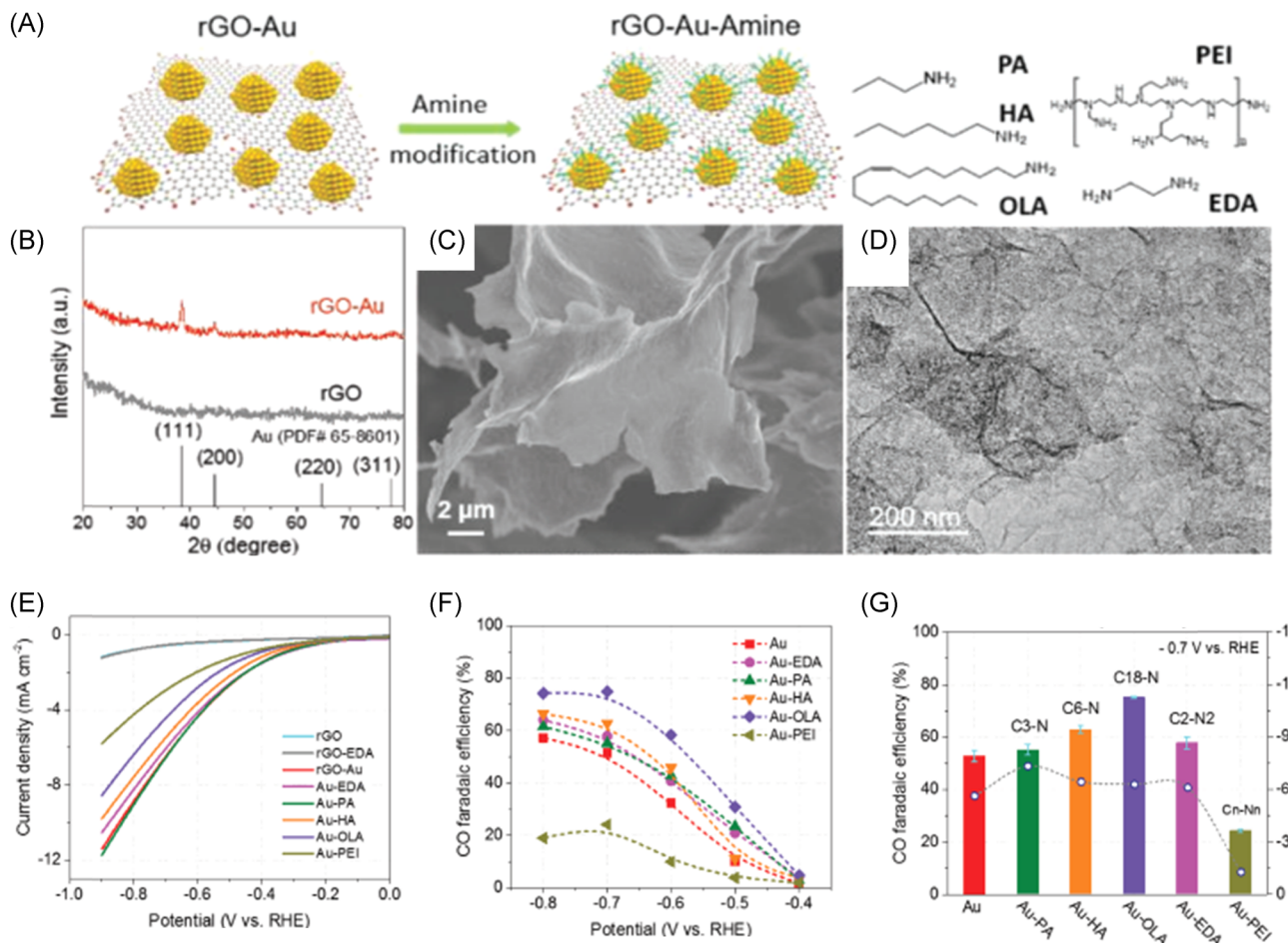
FIGURE 12 A, Schematic of the amine modification on an rGO-Au composite. B, XRD patterns of rGO-Au and rGO. C, SEM and (D) TEM images of rGO-Au, (E) LSV scans of rGO, rGO-EDA, rGO-Au, and Au-amine, (F) FE_{CO} at various potentials for rGO-Au and Au-amine catalysts, and (G) the FE_{CO} (column) and j_{CO} (circle) at −0.7 V. FE, Faradaic efficiency; GO, graphite oxide; LSV, linear sweep voltammetry; SEM, scanning electron microscopy; TEM, transmission electron microscopy; XRD, X-ray diffraction. Reproduced with permission: Copyright 2018, Wiley.[79]

optical properties of graphene via surface modification and engineering of edge strain, surface energy, carrier density, and spins. In addition, to improve the hydrophilicity of the graphene surface, multiple atom doping can be employed as another strategy.[70,71] Boron atoms can be used as a dopant for graphene in plane surface modification, thereby suggesting an increase in spin densities. In addition, B can improve the charge polarization of graphene, thereby enhancing the stability of polarized O in CO_2 atoms. Therefore, B and C charges can provide active sites for CO_2 reduction and facilitate the *COOH absorption to graphene formate. In contrast, the polarization of carbon networks can be induced by N doping, owing to a higher electronegativity of N atoms when compared with C atoms.[72] Further, the transition metal doping of graphene with metals such as Mn, Fe, Al, Au, Ag, and Pt is an efficient way to enhance the CO_2 conversion efficiency. For example, Lv et al[73] investigated

the effect of Ag in wrapped nitrogen-doped carbon-3D graphene foam (Ag-G-NCF) during the electrochemical reduction of CO_2 to ethanol. They used the thermal process to prepare the Ag-G-NCF electrode. As a result, a FE of ~85% was achieved at −0.7 V (vs reversible hydrogen electrode [RHE]) with a high stability during the CO_2 reduction to ethanol; this can be attributed to the strengthening of the binding energy of CO* with the 3D structure of graphene and Ag atom surface (see Figure 9).

3.2 | Surface tuning

Surface tuning is another strategy to modify the graphene surface; this can be done through defect engineering, vertical alignment, and wrapped shape. For example, Han et al[74] demonstrated a method for the defect engineering of graphene surface in CO_2 reduction application.
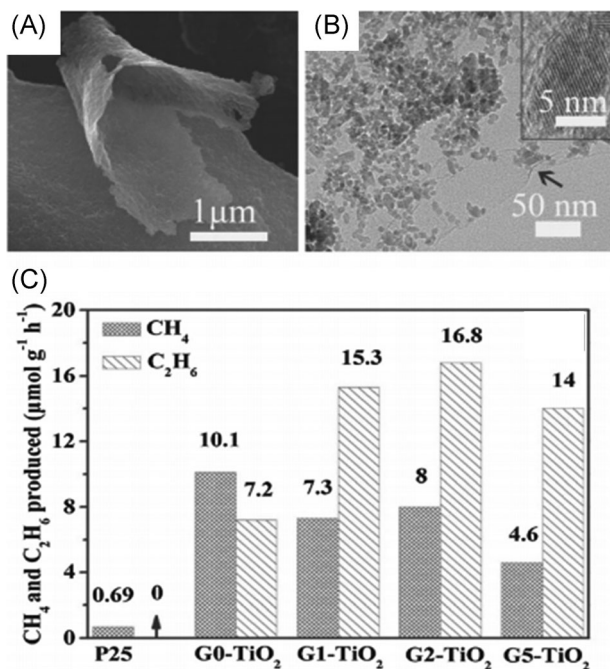
FIGURE 13 A, FESEM and (B) TEM images of graphene/TiO$_2$ hybrid nanosheet composites; C, photocatalytic activity of Gx/TiO$_2$ ($x = 0$, 1, 2, and 5) samples and P25. FE, Faradaic efficiency; SEM, scanning electron microscopy; TEM, transmission electron microscopy. Reproduced with permission: Copyright 2013, Wiley.[87]

This method involves N removal for enhancing the CO$_2$ reaction properties. Figure 10A schematically illustrates the process of producing a defective graphene by using N removal method. As a result, the defective graphene exhibited a high FE of ~84%, which can be ascribed to an increase in active sites and the chemisorption of CO$_2$ caused by defect engineering (see Figure 10B). In addition, the increase in active sites on the graphene surface can be achieved via wrapped shape method as shown in Figure 11.[75] The high CO$_2$ reduction performance of the wrapped shape of graphene can be attributed to an increase in active site networks and a strong interaction between photo-generated hole-electron pairs and the absorbed CO$_2$ molecules on the graphene surface.

3.3 | Composite structure

Several works have been carried out to produce graphene-based composite structures for enhanced CO$_2$ reduction activity. Graphene usually acts as a support for active phases such as NPs and nano-sheets by providing a large surface area. The synergy between the combined structures enhances the charge transport

and helps in easy adsorption of CO$_2$ on the surface of the catalyst.[76]

In electrocatalytic CO$_2$ reduction, graphene has gained extensive interest because of its unique properties such as large surface area, high conductivity, and high stability. In one study, a composite of Cu NP and N-doped graphene was synthesized. Their result revealed that *CO radical transformed into *OC–COH because N-doped carbon promoted ethanol or *n*-propanol generation.[77,78] Moreover, reduced graphene oxide (RGO) was used as a support for gold NPs (~2.4 nm).[79] The synthesized catalyst had a FE ranging between 32% and 60% for the production of CO. In this phenomenon, the defective site of RGO acted as the adsorption site, and some organic solvents were used to further tune the electrocatalytic properties of the synthesized catalyst as shown in Figure 12A. The FE could be increased up to 59% to 75% after the addition of amine groups, which promote CO formation; the FE can be further enhanced by increasing the alkyl chain length as shown in Figure 12B-G.

Similarly, in photocatalytic CO$_2$ reduction, graphene has shown promise as an efficient electron acceptor and transporter. In addition, it reduces the recombination of photo-generated charge carriers.[80-82] Yu et al[83] synthesized a RGO-CdS nano-rod for photocatalytic CO$_2$ reduction, and the structure exhibited an enhanced electron-hole separation because of the high electronic conductivity of RGO. Furthermore, it was found that there is a π–π conjugation interaction between the RGO and CO$_2$ molecules, which plays an important role in making the adsorption easier and activating the CO$_2$ molecules on the surface of the catalyst. In another study, it was found that graphene can tune the size and morphology of a catalyst. Li et al[84] synthesized ZnO NPs on a RGO nano-sheet by using the hydrothermal method. The size of the ZnO NPs was reduced in the composite structure by using RGO as the anchoring site, which reduces self-aggregation. Because of the large surface area of RGO and a uniform distribution of ZnO NPs on the surface, the catalyst exhibited an enhanced production of CH$_3$OH. Moreover, the rational design of graphene demonstrated an enhanced CO$_2$ reduction activity. The 0D-2D and 1D-2D composites of graphene were found to have a smaller contact area and a limited electron transfer when compared with the 2D-2D composite of graphene.[85] For example, Liang et al[86] compared the photocatalytic performance of carbon nanotube/titania nanosheet and graphene/titania nanosheet. The result revealed that the graphene composite exhibited a better performance because of the 2D-2D intimate interfacial contact with the titania nanosheet when compared with the 1D-2D contact with
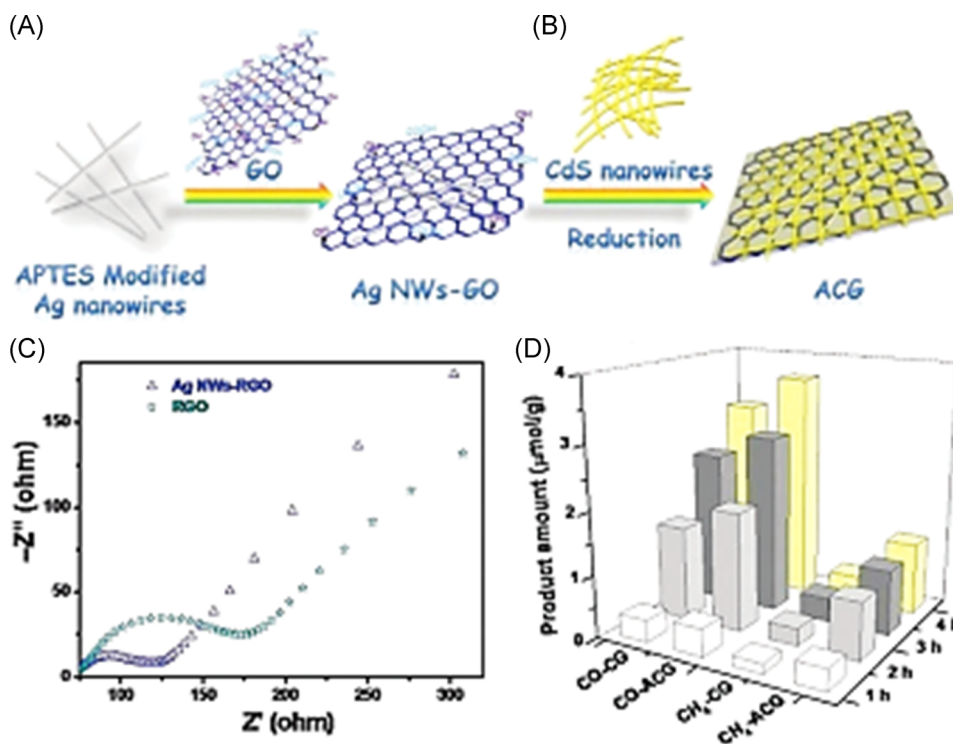
FIGURE 14 A, Schematic of the synthesis of ACG hybrid structure. B, Electrochemical impedance spectroscopy Nyquist diagrams of RGO and Ag NWs-RGO. C, The amounts of CO and CH_4 formed in the photocatalytic reduction of CO_2 in the presence of H_2O vapor over the ACG and RGO-CdS NWs under visible light irradiation. RGO, reduced graphene oxide. Reproduced with permission: Copyright 2015, The Royal Society of Chemistry.[88]

FIGURE 15 A, The advantages of graphene-based catalyst for CO_2 reduction rather than other metal-based catalysts, and (B) strategies for improving the efficiency of graphene-based catalyst for CO_2 reduction

TABLE 1 The recent progress of graphene-based materials in electrochemical CO_2 reduction

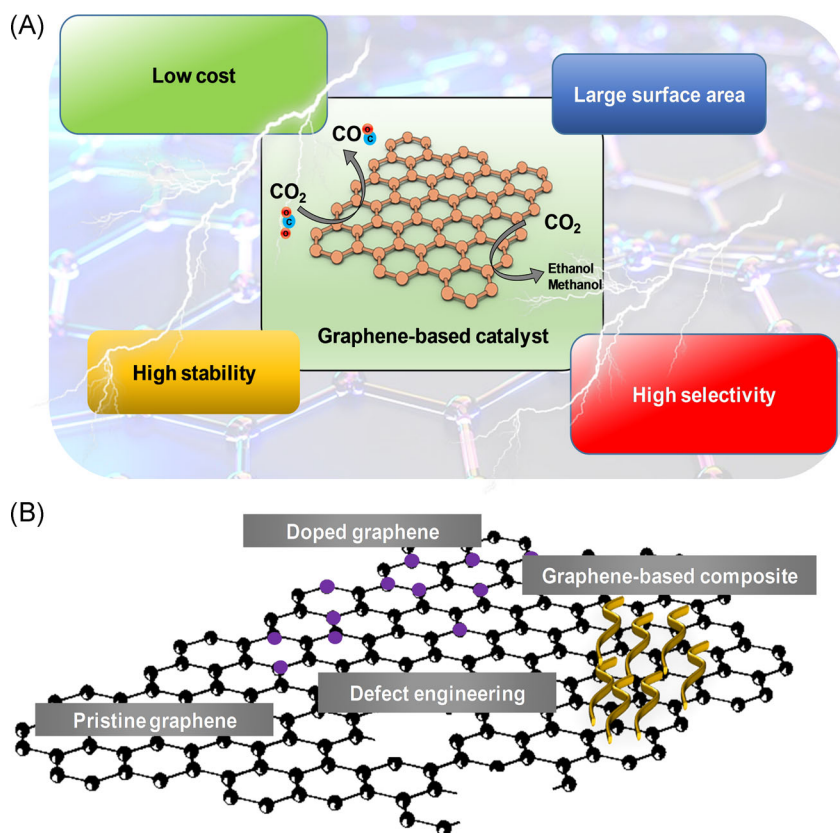| Catalyst	Electrolyte	Product	Onset potential	Faradic efficiency (%)	Stability	Reference
NG foam	0.1 M $KHCO_3$	CO	−0.58 V (vs RHE)	85	5 h	90
NG	0.1 M $KHCO_3$	C_2H_5OH	−0.4 V (vs RHE)	36	–	91
Ni-NG	0.5 M $KHCO_3$	CO	−0.5 V (vs RHE)	95	20 h	92
Pt-NG	0.1 M KNO_3	CH_3OH	−0.3 V (vs RHE)	41	–	93
B-doped Gr	0.1 M $KHCO_3$	HCOOH	−1.4 V (vs RHE)	66	4 h	71
Cu_2O/G	0.5 M $NaHCO_3$	C_2H_5OH	−0.9 V (vs RHE)	9.9	20 min	94
NGQDs	1 M KOH	C_2H_4	−0.75 V (vs RHE)	31	–	95
Cu-rGO	0.1 M $NaHCO_3$	CO	−0.4 V (vs RHE)	21.7	15 h	96
Ag-NG-CF	0.1 M $KHCO_3$	C_2H_5OH	−0.7 V (vs RHE)	85	10 h	73
Fe-NG	0.1 M $KHCO_3$	CO	−0.6 V (vs RHE)	80	10 h	97
Sb-Gr	0.1 M $NaHCO_3$	HCOOH	−1.06 V (vs RHE)	84	12 h	98
PdTe/FLG	0.1 M $KHCO_3$	CO	−0.8 V (vs RHE)	90	5 h	24
Ni_2+@NG	0.5 M $KHCO_3$	CO	−0.68 V (vs RHE)	92	20 h	99

Abbreviation: RHE, reversible hydrogen electrode.

the carbon nanotube. In addition, Tu et al[87] investigated the 2D sandwich like composite structure of graphene and TiO_2. The 2D contact facilitates the charge separation and enhances the photocatalytic efficiency. The TiO_2 NPs were uniformly distributed, and the transfer of photo-generated electrons from TiO_2 to graphene sheets was enhanced. The graphene/TiO_2 nanocomposite shows a much better performance than the bare TiO_2 in the production of C_2H_6 and CH_4 as shown in Figure 13. Similarly, a ternary composite of graphene also shows an enhanced performance toward photocatalytic CO_2 reduction. In one study, Liu et al[88] synthesized an Ag NWs-RGO-CdS NWs (ACG) composite via a simple electrostatic self-assembly method followed by a hydrothermal reduction process. As shown in Figure 14A, the addition of Ag nanowires increases the conductivity of RGO, which results in a better separation and transfer of charge carriers than the RGO-CdS nanowire catalyst. As a result, the ternary composite exhibited an enhanced performance in the production of CO and CH_4 than the RGO-CdS catalyst, as shown in Figure 14B,C.

4 | CONCLUSION AND OUTLOOK

CO_2 reduction is an extremely promising research field because of the high demand for reduction of CO_2 that is caused by the global warming and conversion of CO_2 into a useful energy. Figure 15A illustrates the merit of graphene-based catalyst for CO_2 reduction rather than other metal-based catalysts, schematically. Graphene-based catalysts are a remarkable candidate for the photo-electrochemical reduction of CO_2. Because pristine graphene is inactive, the catalytic properties of graphene-based materials have to be improved by different strategies such as doping, producing composites, wrapping shapes, and defect engineering.[89] In this review, we first investigated the fundamentals of CO_2 reduction, and subsequently studied the recent progress in the graphene-based catalysts for CO_2 reduction. Furthermore, different strategies used to modify the graphene-based materials for CO_2 conversion were investigated (see Figure 15B).

The electron transfer can be enhanced by changing the structure of graphene-based materials, suggesting an enhancement of catalytic properties. There are different strategies for the efficient design of graphene-based materials, including doping, defect engineering, controlling a number of layers and thicknesses.[1] Besides, developing some characterization methods may lead to developing the design of theoretical models to a deep understanding of catalytic reactions and correlation within intermediates. Therefore, the corporation of experiment and theory will help us to design high efficient catalysts and enhancing the number of active sites. Moreover, the discovery of earth-abundant and low-cost catalysts such as 2D materials that can reduce CO_2 to useful products with high efficiency could be a focus of study and research to design of novel catalysts. Furthermore, design of NPs and lateral and van der Walls heterostructure provide a remarkable tuning over the mechanical and electronic features, suggesting create a various catalytic applications.[1-5]
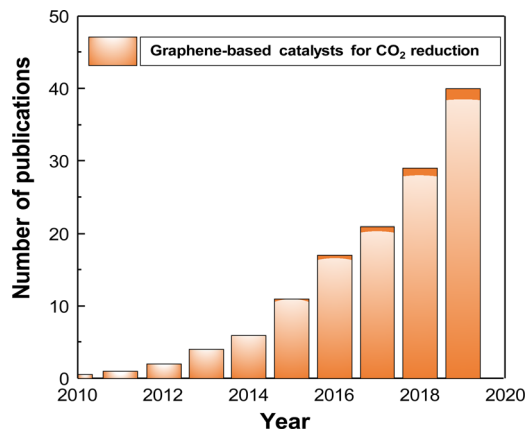
FIGURE 16 The number of publications per year on graphene-based catalysts for CO_2 reduction from 2010 to 2019. The publication search was carried out via the Web of Science provided by Thomson Reuters

Table 1 shows the recent progress of graphene-based materials in electro-catalytic CO_2 reduction. Metal doping of graphene can increase the number of active sites for electrochemical CO_2 reduction; this improvement can be ascribed to an increase in charge and spin density caused by an increase in adsorption sites of CO_2 molecules. Moreover, the defect engineering of the graphene surface can uniformly distribute the local charge density and enhance the affinity for the reaction of intermediates.

Despite outstanding progress in CO_2 reduction via graphene-based materials, the efficient generation of certain compounds remains a huge challenge. Further development in the formation of new products and an increase in the selectivity of graphene-based materials for CO_2 reduction are likely to be achieved with a new design of electrode structure and electrolyte.

Recently, the number of publications regarding the graphene-based catalysts for CO_2 reduction has been reported. Figure 16 indicates the number of publications per year on graphene-based catalysts for CO_2 reduction from 2010 to 2019. This survey was carried out via the Web of Science provided by Thomson Reuters. The research on the graphene-based catalysts for CO_2 reduction increased dramatically, reaching about 40 publications in 2019. This trend shows graphene-based catalyst has a remarkable potential to be utilized in energy conversion, shortly.

Graphene-based catalysts provide a tunable interface for CO_2 reduction and optimize the interaction between the absorbed CO_2 molecules on the graphene surface and the intermediates. The study on the physical and mechanical properties of graphene-based catalysts would be a new field of research in the application of CO_2 reduction. In addition, the microscopic methods can provide a deep understanding of the CO_2 reduction mechanism.

ORCID

Soo Young Kim http://orcid.org/0000-0002-0685-7991

REFERENCES

1. Hasani A, Tekalgne M, Van Le Q, Jang HW, Kim SY. Two-dimensional materials as catalysts for solar fuels: hydrogen evolution reaction and CO_2 reduction. *J Mater Chem A*. 2019;7: 430-454.
2. McCollum D, Bauer N, Calvin K, Kitous A, Riahi K. Fossil resource and energy security dynamics in conventional and carbon-constrained worlds. *Clim Change*. 2014;123:413-426.
3. Olah GA. Beyond oil and gas: the methanol economy. *Angew Chem Int Ed*. 2005;44:2636-2639.
4. Vasileff A, Xu C, Jiao Y, Zheng Y, Qiao S-Z. Surface and interface engineering in copper-based bimetallic materials for selective CO_2 electroreduction. *Chem*. 2018;4:1809-1831.
5. Jiao Y, Zheng Y, Chen P, Jaroniec M, Qiao S-Z. Molecular scaffolding strategy with synergistic active centers to facilitate electrocatalytic CO_2 reduction to hydrocarbon/alcohol. *J Am Chem Soc*. 2017;139:18093-18100.
6. Liu J, Guo C, Vasileff A, Qiao S. Nanostructured 2D materials: prospective catalysts for electrochemical CO_2 reduction. *Small Methods*. 2017;1:1600006.
7. Lee CW, Yang KD, Nam DH, et al. Defining a materials database for the design of copper binary alloy catalysts for electrochemical CO_2 conversion. *Adv Mater*. 2018;30:1704717.
8. Wang Z-L, Li C, Yamauchi Y. Nanostructured nonprecious metal catalysts for electrochemical reduction of carbon dioxide. *Nano Today*. 2016;11:373-391.
9. Spataru N, Tokuhiro K, Terashima C, Rao TN, Fujishima A. Electrochemical reduction of carbon dioxide at ruthenium dioxide deposited on boron-doped diamond. *J Appl Electrochem*. 2003;33:1205-1210.
10. Bandi A. Electrochemical reduction of carbon dioxide on conductive metallic oxides. *J Electrochem Soc*. 1990;137:2157-2160.
11. Sun X, Zhu Q, Kang X, et al. Molybdenum–bismuth bimetallic chalcogenide nanosheets for highly efficient electrocatalytic reduction of carbon dioxide to methanol. *Angew Chem Int Ed*. 2016;55:6771-6775.
12. Back S, Jung Y. TiC and TiN-supported single-atom catalysts for dramatic improvements in CO_2 electrochemical reduction to CH_4. *ACS Energy Lett*. 2017;2:969-975.
13. Wang Y, Hou P, Wang Z, Kang P. Zinc imidazolate metal–organic frameworks (ZIF-8) for electrochemical reduction of CO_2 to CO. *ChemPhysChem*. 2017;18:3142-3147.
14. Zhang Y, Tan Y-W, Stormer HL, Kim P. Experimental observation of the quantum Hall effect and Berry's phase in graphene. *Nature*. 2005;438:201-204.
15. Berger C. Electronic confinement and coherence in patterned epitaxial graphene. *Science*. 2006;312:1191-1196.
16. Ghosh S, Calizo I, Teweldebrhan D, et al. Extremely high thermal conductivity of graphene: prospects for thermal management applications in nanoelectronic circuits. *Appl Phys Lett*. 2008;92:151911.

17. Stoller MD, Park S, Zhu Y, An J, Ruoff RS. Graphene-based ultracapacitors. *Nano Lett.* 2008;8:3498-3502.

18. Novoselov KS. Electric field effect in atomically thin carbon films. *Science.* 2004;306:666-669.

19. Tung VC, Allen MJ, Yang Y, Kaner RB. High-throughput solution processing of large-scale graphene. *Nat Nanotechnol.* 2009;4:25-29.

20. Choucair M, Thordarson P, Stride JA. Gram-scale production of graphene based on solvothermal synthesis and sonication. *Nat Nanotechnol.* 2009;4:30-33.

21. Kim KS, Zhao Y, Jang H, et al. Large-scale pattern growth of graphene films for stretchable transparent electrodes. *Nature.* 2009;457:706-710.

22. Wu T, Lin J, Cheng Y, et al. Porous Graphene-Confined Fe–K as Highly Efficient Catalyst for CO_2 Direct Hydrogenation to Light Olefins. *ACS Appl Mater Interfaces.* 2018; 10:23439-23443.

23. Ning H, Mao Q, Wang W, et al. N-doped reduced graphene oxide supported Cu_2O nanocubes as high active catalyst for CO_2 electroreduction to C_2H_4. *J Alloys Compd.* 2019;785:7-12.

24. Tao H, Sun X, Back S, et al. Doping palladium with tellurium for the highly selective electrocatalytic reduction of aqueous CO_2 to CO. *Chem Sci.* 2018;9:483-487.

25. Zhang N, Yang M-Q, Liu S, Sun Y, Xu Y-J. Waltzing with the versatile platform of graphene to synthesize composite photocatalysts. *Chem Rev.* 2015;115:10307-10377.

26. Yang M-Q, Zhang N, Pagliaro M, Xu Y-J. Artificial photosynthesis over graphene–semiconductor composites. *Chem Soc Rev.* 2014;43:8240-8254.

27. Sun Z, Ma T, Tao H, Fan Q, Han B. Fundamentals and challenges of electrochemical CO_2 reduction using two-dimensional materials. *Chem.* 2017;3:560-587.

28. Kauffman DR, Thakkar J, Siva R, et al. Efficient electrochemical CO_2 conversion powered by renewable energy. *ACS Appl Mater Interfaces.* 2015;7:15626-15632.

29. Durst J, Rudnev A, Dutta A, et al. Electrochemical CO_2 reduction: a critical view on fundamentals, materials and applications. *CHIMIA International Journal for Chemistry.* 2015;69: 769-776.

30. Sun Z, Talreja N, Tao H, et al. Catalysis of carbon dioxide photoreduction on nanosheets: fundamentals and challenges. *Angew Chem Int Ed.* 2018;57:7610-7627.

31. Schneider J, Jia H, Muckerman JT, Fujita E. Thermodynamics and kinetics of CO_2, CO, and H+ binding to the metal centre of CO_2 reduction catalysts. *Chem Soc Rev.* 2012; 41:2036-2051.

32. Geioushy R, Khaled MM, Alhooshani K, Hakeem AS, Rinaldi A. Graphene/ZnO/Cu_2O electrocatalyst for selective conversion of CO_2 into n-propanol. *Electrochim Acta.* 2017;245: 456-462.

33. Thorson MR, Siil KI, Kenis PJ. Effect of cations on the electrochemical conversion of CO_2 to CO. *J Electrochem Soc.* 2012; 160:F69-F74.

34. Ogura K, Ferrell JR III, Cugini AV, Smotkin ES, Salazar-Villalpando MD. CO_2 attraction by specifically adsorbed anions and subsequent accelerated electrochemical reduction. *Electrochim Acta.* 2010;56:381-386.

35. Vassiliev YB, Bagotzky V, Khazova O, Mayorova N. Electroreduction of carbon dioxide: part II. The mechanism of reduction in aprotic solvents. *J Electroanal Chem Interf Electrochem.* 1985;189:295-309.

36. Sun X, Kang X, Zhu Q, et al. Very highly efficient reduction of CO_2 to CH_4 using metal-free N-doped carbon electrodes. *Chem Sci.* 2016;7:2883-2887.

37. Ma T, Fan Q, Li X, Qiu J, Wu T, Sun Z. Graphene-based materials for electrochemical CO_2 reduction. *J CO2 Uti.* 2019;30: 168-182.

38. Feng Y, Li Z, Liu H, et al. Laser-prepared CuZn alloy catalyst for selective electrochemical reduction of CO_2 to ethylene. *Langmuir.* 2018;34:13544-13549.

39. Kang X, Zhu Q, Sun X, et al. Highly efficient electrochemical reduction of CO_2 to CH_4 in an ionic liquid using a metal–organic framework cathode. *Chem Sci.* 2016;7:266-273.

40. Bevilacqua M, Filippi J, Miller HA, Vizza F. Recent technological progress in CO_2 electroreduction to fuels and energy carriers in aqueous environments. *Energy Technol.* 2015;3:197-210.

41. Bevilacqua M, Filippi J, Lavacchi A, et al. Energy savings in the conversion of CO_2 to fuels using an electrolytic device. *Energy Technol.* 2014;2:522-525.

42. Hori Y, Wakebe H, Tsukamoto T, Koga O. Electrocatalytic process of CO selectivity in electrochemical reduction of CO_2 at metal electrodes in aqueous media. *Electrochim Acta.* 1994;39: 1833-1839.

43. Chernyshova IV, Somasundaran P, Ponnurangam S. On the origin of the elusive first intermediate of CO_2 electroreduction. *PNAS.* 2018;115:E9261-E9270.

44. Kai T, Zhou M, Duan Z, Henkelman GA, Bard AJ. Detection of $CO_2^{\bullet-}$ in the electrochemical reduction of carbon dioxide in N, N-dimethylformamide by scanning electrochemical microscopy. *J Am Chem Soc.* 2017;139:18552-18557.

45. McQuillan A, Hendra P, Fleischmann M. Raman spectroscopic investigation of silver electrodes. *J Electroanal Chem.* 1975;65: 933-944.

46. Yoo JS, Christensen R, Vegge T, Nørskov JK, Studt F. Theoretical insight into the trends that guide the electrochemical reduction of carbon dioxide to formic acid. *ChemSusChem.* 2016;9:358-363.

47. Chai G-L, Guo Z-X. Highly effective sites and selectivity of nitrogen-doped graphene/CNT catalysts for CO_2 electrochemical reduction. *Chem Sci.* 2016;7:1268-1275.

48. Kortlever R, Shen J, Schouten KJP, Calle-Vallejo F, Koper MT. Catalysts and reaction pathways for the electrochemical reduction of carbon dioxide. *J Phys Chem Lett.* 2015;6:4073-4082.

49. Peterson AA, Abild-Pedersen F, Studt F, Rossmeisl J, Nørskov JK. How copper catalyzes the electroreduction of carbon dioxide into hydrocarbon fuels. *Energy Environ Sci.* 2010;3:1311-1315.

50. Zheng T, Jiang K, Wang H. Recent advances in electrochemical CO_2-to-CO conversion on heterogeneous catalysts. *Adv Mater.* 2018;30:1802066.

51. Han Z, Choi C, Tao H, et al. Tuning the Pd-catalyzed electroreduction of CO_2 to CO with reduced overpotential. *Catal Sci.* 2018;8:3894-3900.

52. Gao K, Jo SB, Shi X, et al. Over 12% efficiency nonfullerene all-small-molecule organic solar cells with sequentially evolved multilength scale morphologies. *Adv Mater.* 2019;31:1807842.

53. Varela AS, Ju W, Strasser P. Molecular nitrogen–carbon catalysts, solid metal organic framework catalysts, and solid

metal/nitrogen-doped carbon (MNC) catalysts for the electrochemical CO₂ reduction. *Adv Energy Mater.* 2018;8:1802905.

54. Duan X, Xu J, Wei Z, et al. Metal-free carbon materials for CO₂ electrochemical reduction. *Adv Mater.* 2017;29:1701784.

55. Jia M, Choi C, Wu T-S, et al. Carbon-supported Ni nanoparticles for efficient CO₂ electroreduction. *Chem Sci.* 2018;9: 8775-8780.

56. Xiang Q, Yu J. Graphene-based photocatalysts for hydrogen generation. *J Phys Chem Lett.* 2013;4:753-759.

57. Liu S, Yu J, Jaroniec M. Anatase TiO₂ with dominant high-energy {001} facets: synthesis, properties, and applications. *Chem Mater.* 2011;23:4085-4093.

58. Zhang J, Yu J, Jaroniec M, Gong JR. Noble metal-free reduced graphene oxide-ZnxCd1−xS nanocomposite with enhanced solar photocatalytic H₂-production performance. *Nano Lett.* 2012; 12:4584-4589.

59. Han TH, Lee WJ, Lee DH, Kim JE, Choi EY, Kim SO. Peptide/graphene hybrid assembly into core/shell nanowires. *Adv Mater.* 2010;22:2060-2064.

60. Yuan W, Yuan J, Zhou M, Pan C. Synthesis, characterization, and fluorescence of pyrene-containing eight-arm star-shaped dendrimer-like copolymer with pentaerythritol core. *J Polym Sci, Part A: Polym Chem.* 2008;46:2788-2798.

61. Yang Y, Zhang Y-M, Chen Y, Zhao D, Chen JT, Liu Y. Construction of a graphene oxide based noncovalent multiple nanosupramolecular assembly as a scaffold for drug delivery. *Chem Eur J.* 2012;18:4208-4215.

62. Raghu AV, Lee YR, Jeong HM, Shin CM. Preparation and physical properties of waterborne polyurethane/functionalized graphene sheet nanocomposites. *Macromol Chem Phys.* 2008; 209:2487-2493.

63. Liang J, Huang Y, Zhang L, et al. Molecular-level dispersion of graphene into poly(vinyl alcohol) and effective reinforcement of their nanocomposites. *Adv Funct Mater.* 2009;19:2297-2302.

64. Kim H, Miura Y, Macosko CW. Graphene/polyurethane nanocomposites for improved gas barrier and electrical conductivity. *Chem Mater.* 2010;22:3441-3450.

65. Lerf A, He H, Forster M, Klinowski J. Structure of graphite oxide revisited. *J Phys Chem B.* 1998;102:4477-4482.

66. Stankovich S, Piner RD, Nguyen ST, Ruoff RS. Synthesis and exfoliation of isocyanate-treated graphene oxide nanoplatelets. *Carbon.* 2006;44:3342-3347.

67. Jiang B, Qu Y, Zhang L, Liang Z, Zhang Y. 4-Mercaptophenylboronic acid functionalized graphene oxide composites: preparation, characterization and selective enrichment of glycopeptides. *Anal Chim Acta.* 2016;912:41-48.

68. Chen L, Zhong X, Yi X, et al. Radionuclide 131I labeled reduced graphene oxide for nuclear imaging guided combined radio- and photothermal therapy of cancer. *Biomaterials.* 2015;66:21-28.

69. Peng X, He C, Liu J, Wang H. Biomimetic jellyfish-like PVA/graphene oxide nanocomposite hydrogels with anisotropic and pH-responsive mechanical properties. *J Mater Sci.* 2016;51: 5901-5911.

70. Hao G-P, Sahraie NR, Zhang Q, et al. Hydrophilic non-precious metal nitrogen-doped carbon electrocatalysts for enhanced efficiency in oxygen reduction reaction. *Chem Commun.* 2015;51: 17285-17288.

71. Sreekanth N, Nazrulla MA, Vineesh TV, Sailaja K, Phani KL. Metal-free boron-doped graphene for selective electroreduction of carbon dioxide to formic acid/formate. *Chem Commun.* 2015;51:16061-16064.

72. Tao H, Yan C, Robertson AW, et al. N-Doping of graphene oxide at low temperature for the oxygen reduction reaction. *Chem Commun.* 2017;53:873-876.

73. Lv K, Fan Y, Zhu Y, et al. Elastic Ag-anchored N-doped graphene/carbon foam for the selective electrochemical reduction of carbon dioxide to ethanol. *J Mater Chem A.* 2018;6: 5025-5031.

74. Han P, Yu X, Yuan D, et al. Defective graphene for electrocatalytic CO₂ reduction. *J Colloid Interface Sci.* 2019;534: 332-337.

75. Rambabu Y, Kumar U, Singhal N, et al. Photocatalytic reduction of carbon dioxide using graphene oxide wrapped TiO₂ nanotubes. *Appl Surf Sci.* 2019;485:48-55.

76. Navalon S, Dhakshinamoorthy A, Alvaro M, Garcia H. Metal nanoparticles supported on two-dimensional graphenes as heterogeneous catalysts. *Coord Chem Rev.* 2016;312:99-148.

77. Song Y, Peng R, Hensley DK, et al. High-selectivity electrochemical conversion of CO₂ to ethanol using a copper nanoparticle/N-doped graphene electrode. *ChemistrySelect.* 2016;1:6055-6061.

78. Li Y, Su H, Chan SH, Sun Q. CO₂ electroreduction performance of transition metal dimers supported on graphene: a theoretical study. *ACS Catal.* 2015;5:6658-6664.

79. Zhao Y, Wang C, Liu Y, MacFarlane DR, Wallace GG. Engineering surface amine modifiers of ultrasmall gold nanoparticles supported on reduced graphene oxide for improved electrochemical CO₂ reduction. *Adv Energy Mater.* 2018;8:1801400.

80. Tu W, Zhou Y, Zou Z. Versatile graphene-promoting photocatalytic performance of semiconductors: basic principles, synthesis, solar energy conversion, and environmental applications. *Adv Funct Mater.* 2013;23:4996-5008.

81. Fresno F, Portela R, Suárez S, Coronado JM. Photocatalytic materials: recent achievements and near future trends. *J Mater Chem A.* 2014;2:2863-2884.

82. Izumi Y. Recent advances in the photocatalytic conversion of carbon dioxide to fuels with water and/or hydrogen using solar energy and beyond. *Coord Chem Rev.* 2013;257:171-186.

83. Yu J, Jin J, Cheng B, Jaroniec M. A noble metal-free reduced graphene oxide–CdS nanorod composite for the enhanced visible-light photocatalytic reduction of CO₂ to solar fuel. *J Mater Chem A.* 2014;2:3407-3416.

84. Li X, Wang Q, Zhao Y, Wu W, Chen J, Meng H. Green synthesis and photo-catalytic performances for ZnO-reduced graphene oxide nanocomposites. *J Colloid Interface Sci.* 2013; 411:69-75.

85. Low J, Cao S, Yu J, Wageh S. Two-dimensional layered composite photocatalysts. *Chem Commun.* 2014;50:10768-10777.

86. Liang YT, Vijayan BK, Lyandres O, Gray KA, Hersam MC. Effect of dimensionality on the photocatalytic behavior of carbon–titania nanosheet composites: charge transfer at nanomaterial interfaces. *J Phys Chem.* 2012;3:1760-1765.

87. Tu W, Zhou Y, Liu Q, et al. An in situ simultaneous reduction-hydrolysis technique for fabrication of TiO₂-graphene 2D sandwich-like hybrid nanosheets: graphene-promoted selectivity of photocatalytic-driven hydrogenation and coupling of CO₂ into methane and ethane. *Adv Funct Mater.* 2013;23: 1743-1749.

88. Liu S, Weng B, Tang Z-R, Xu Y-J. Constructing one-dimensional silver nanowire-doped reduced graphene oxide integrated with CdS nanowire network hybrid structures toward artificial photosynthesis. *Nanoscale*. 2015;7:861-866.

89. Choi S, Kim C, Suh JM, Jang HW. Reduced graphene oxide-based materials for electrochemical energy conversion reactions. *Carbon Energy*. 2019;1:85-108.

90. Wu J, Liu M, Sharma PP, et al. Incorporation of nitrogen defects for efficient reduction of CO_2 via two-electron pathway on three-dimensional graphene foam. *Nano Lett*. 2015;16:466-470.

91. Yuan J, Zhi W-Y, Liu L, Yang MP, Wang H, Lu JX. Electrochemical reduction of CO_2 at metal-free N-functionalized graphene oxide electrodes. *Electrochim Acta*. 2018;282:694-701.

92. Jiang K, Siahrostami S, Zheng T, et al. Isolated Ni single atoms in graphene nanosheets for high-performance CO_2 reduction. *Energy Environ Sci*. 2018;11:893-903.

93. Ensafi AA, Alinajafi HA, Rezaei B. Pt-modified nitrogen doped reduced graphene oxide: a powerful electrocatalyst for direct CO_2 reduction to methanol. *J Electroanal Chem*. 2016;783:82-89.

94. Geioushy RA, Khaled MM, Hakeem AS, Alhooshani K, Basheer C. High efficiency graphene/Cu_2O electrode for the electrochemical reduction of carbon dioxide to ethanol. *J Electroanal Chem*. 2017;785:138-143.

95. Wu J, Ma S, Sun J, et al. A metal-free electrocatalyst for carbon dioxide reduction to multi-carbon hydrocarbons and oxygenates. *Nat Commun*. 2016;7:13869.

96. Hossain MN, Wen J, Chen A. Unique copper and reduced graphene oxide nanocomposite toward the efficient electrochemical reduction of carbon dioxide. *Sci Rep*. 2017;7:3184.

97. Zhang C, Yang S, Wu J, et al. Electrochemical CO_2 reduction with atomic iron-dispersed on nitrogen-doped graphene. *Adv Energy Mater*. 2018;8:1703487.

98. Li F, Xue M, Li J, et al. Unlocking the electrocatalytic activity of antimony for CO_2 reduction by two-dimensional engineering of the bulk material. *Angew Chem Int Ed*. 2017;56:14718-14722.

99. Bi W, Li X, You R, et al. Surface immobilization of transition metal ions on nitrogen-doped graphene realizing high-efficient and selective CO_2 reduction. *Adv Mater*. 2018;30:1706617.

AUTHOR BIOGRAPHIES

Amirhossein Hasani received his BSc and MSc in Electronic Engineering from Sadjad University of Technology and KN Toosi University of Technology in 2011 and 2014, respectively. He is currently PhD candidate at the school of Chemical Engineering and Material Science in Chung-Ang University, Seoul, South Korea. His research interests include the fabrication of two dimensional materials, quantum dots and metal oxides and its applications in energy devices, photo-electrochemical water splitting smart windows, thin film transistors, solar cells, and gas sensors.

Soo Young Kim is a professor in the Department of Materials Science and Engineering in Korea University. He received the BS, MS, and PhD degrees in materials science and engineering from Pohang University of Science and Technology (POSTECH). He combined his experience about optoelectronic devices with two-dimensional and nano materials so that his research is focused on the optimization of two-dimensional materials and organo/inorgano halides' properties and their application to energy devices, such as organic photovoltaics, perovskite solar cells, organic light emitting diodes, gas sensors, hydrogen evolution reaction, and CO_2 reduction.